Mobility of organic compounds in a soft clay-rich rock (Tégulines clay, France)

Ning Guo, Zoé Disdier, Emilie Thory, Jean-Charles Robinet, Romain Dagnelie

Mobility of organic compounds in a soft clay-rich rock (Tégulines clay, France)

Ning Guo [a], Zoé Disdier [a], Émilie Thory [a],

Jean-Charles Robinet [b], Romain V.H. Dagnelie [a, *]

(a) Université Paris-Saclay, CEA, Service d'Étude du Comportement des Radionucléides, 91191, Gif-sur-Yvette, France

(b) Andra, R&D Division, parc de la Croix Blanche, 92298, Châtenay-Malabry, France

* Corresponding author. Université Paris-Saclay, CEA/DES/ISAS/DPC/SECR/L3MR, 91191, Gif-sur-Yvette, France.

E-mail address: romain.dagnelie@cea.fr

Abstract

The migration of organic compounds in soils is a major concern in several environmental issues. Contaminants display distinct behaviours as regards to their specific affinities towards soils constituents. The retention mechanism of hydrophobic compounds by natural organic matter is well known. The retention of ionizable compounds is mainly related to oxides and clay minerals, even if less documented in reductive media. In this work, we investigated the migration of organic compounds in a soft clay-rich sedimentary rock (Tégulines clay, France). The aim was to determine the relative contributions of natural sorbents on retention, and eventual correlations with solutes properties. Both hydrophobic compounds (toluene, benzene, naphthalene) and hydrophilic species (adipate, oxalate, ortho-phthalate, benzoate) were investigated, using batch and diffusion experiments.

The retention of neutral aromatic compounds correlates with their lipophilicity (log P_{OW}), confirming that absorption mechanism prevails, despite a low content of natural organic matter (≤ 0.5%). A low retention of ionizable compounds was quantified on Tégulines clay. The eventual discrepancies between data acquired on crushed rock and solid samples are discussed. Low effective diffusion coefficients are quantified. These values hint on the relative contributions of steric and electrostatic exclusion, despite a large pore size in such "soft" clay-rock. Overall, the dataset illustrates a general scheme for assessing the migration over a wide variety of organic compounds. This approach may be useful for predictive modelling of the fate of organic compounds in environmental media.

Keywords:

Clay rock, Organic compound, Adsorption, Absorption, Diffusion, Anion exclusion

Abbreviations and notations:

α: Apparent porosity, accessible during diffusion of reactive solutes

ε: Porosity of media, accessible during diffusion of inert solutes, e.g. H_2O

Π: Exclusion factor from porous media quantified during diffusion

COx: Callovian-Oxfordian (Clay rock)

D_0: Diffusion coefficient (m^2 s^{-1}) in water

D_e: Effective diffusion coefficient (m^2 s^{-1}) in porous media

f_{OM} / f_{CM}: Massic fraction of organic matter / clay minerals in sorbents

HDO: Semi-heavy water

IS: Ionic strength

K_{CM}: Contribution of clay minerals to the solid-liquid distribution coefficient (L kg(clay)$^{-1}$)

K_{OC}: Contribution of organic matter to the solid-liquid distribution coefficient (L kg(NOM)$^{-1}$)

NOM: natural organic matter

OPA: Opalinus (clay rock)

Orga: Organic (compound / sorbate)

P_{APP}: Apparent octanol water partition coefficient

P_{OW}: Octanol water partition coefficient (analogue to K_{OW})

R_d: Solid-liquid distribution coefficient (L kg^{-1})

1. Introduction

The transport of organic compounds in environmental media is studied for various applications: extraction of fossil fuels, fate of emerging organic contaminants, waste disposal and remediation of soils. The term “organic” may be misleading, as it corresponds to a large diversity of compounds: small ionizable compounds such as amino-acids, hydrophobic or hydrophilic hydrocarbons, large synthetic or natural geopolymers and natural organic matter (NOM) such as fulvic and humic acids. This work focuses on the transport of small soluble molecules in the near surface of geological systems. Both ionizable carboxylic acids and neutral aromatic compounds are investigated. The migration of such solutes in sedimentary rocks is highly sensitive to sorption leading to diffusive retardation (Altmann et al., 2012; Shackelford and Moore, 2013). Sorption-influenced transport is largely described in literature for organic compounds (Borisover and Davis, 2015; Schaffer and Licha, 2015) indicating that the retention part may originate from various mechanisms. Hydrophobic compounds, such as alkanes and aromatic compounds are mainly absorbed by NOM (Borisover and Graber, 1997; Karickhoff, 1981) with Freundlich-type sorption isotherm, eventually leading to intra-particulate slow diffusion mechanism (Pignatello and Xing, 1996). On contrary, hydrophilic compounds such as ionizable molecules are adsorbed on the surfaces of minerals, e.g. clays and oxides (Gu et al., 1994; Hwang et al., 2007; Johnson et al., 2004; Kang and Xing, 2007). Adsorption may be assumed in this case, with instantaneous and reversible Langmuir-type isotherms, leading to increased apparent porosity and diffusive retardation factor. Both mechanisms of adsorption and absorption, may occur simultaneously on the various mineralogical components of a natural medium, but the relative contribution of these mechanisms is rarely discussed.

Clay rock geological formations are considered in several countries for hosting a radioactive waste disposal, e.g. Callovian-Oxfordian (COx) and Tégulines in France, Opalinus Clay (OPA) and Helvetic Marl in Switzerland, Boom Clay in Belgium, etc. (Altmann et al., 2012; Appelo et al., 2010; Maes et al., 2011). The COx clay rock has been extensively studied in the context of the French Geological Radioactive Waste Disposal (Cigéo project). Corresponding studies investigated the interaction between inorganic or organic solutes and COx clay rock (Descostes et al., 2008; Melkior et al., 2007; Rasamimanana, 2017a; Savoye et al., 2012). Absorption of neutral hydrophobic compounds occurs in NOM (Vinsot et al., 2017), with an eventual contribution from clay minerals (Willemsen et al., 2019). Similarly, the adsorption of organic anions occurs on clayey minerals, despite a positive charge on clayey mineral surfaces (Rasamimanana et al., 2017b). Still, electrostatic interactions between mineral surfaces and solutes leads to a partial exclusion of anions from rock porosity. This so-called "anion exclusion" decreases both effective diffusion coefficient and retardation factor of anions, as compared to neutral solutes (Chen et al., 2018; Dagnelie et al., 2018). However, some major discrepancies are observed between data measured by sorption on crushed clay rock and retardation factor observed in solid samples. For that reason, the quantification of diffusive retardation factors seems mandatory.

This work focuses on the Tégulines clay, from the Albian Gault geological formation (East Paris Basin, France) under investigation for a potential near surface geological radioactive waste repository (Lerouge et al., 2018; Missana et al., 2017). This repository would confine low-activity long-lived waste, such as ^{14}C-graphite, remain from old natural uranium graphite gas nuclear power reactor, developed in France until the 90s. In absence of exhaustive characterization, the organic source term potentially released by radiolytic

93 lixiviation of graphite waste makes both neutral and anionic reference compounds being of
94 interest (Andra, 2015; Pageot et al., 2016, 2018; Poncet and Petit, 2013). The purpose of this
95 work is to quantify sorption and retardation factors of various organic species, in order to
96 assess the confinement properties of the geological barrier toward potential release of ^{14}C
97 bearing compounds. To that aim, diffusion experiments were performed and compared to
98 sorption experiments or predictive model based on media mineralogy. Moreover, the
99 comparison between results on Tégulines "soft" clay rock and COx "hard" clay rocks,
100 displaying variable compaction, are interesting to assess potential porosity exclusion and
101 effects on sorption-influenced transport of anions.
102
103 **2. Material and methods**
104 **2.1. Rock samples**
105 Experiments were carried out on Tégulines clay samples from the Albian Gault clay
106 formation. Rock samples were collected from two boreholes (AUB01918, AUB01825). The
107 cores were drilled at depths -20 and -22 m from the surface of the studied area (NE-SW) in
108 the eastern part of the Paris Basin (France) (Amédro et al., 2017; Lerouge et al., 2018 and
109 2020). The mineralogical composition is detailed in supplementary data (Table S1). It is
110 basically composed of 50% of clay minerals, 40% of quartz, less than 5% of calcite and 0.6%
111 of NOM. After drilling, the core samples were protected from oxygen using container with
112 $N_{2(g)}$. They were manipulated inside a glovebox (P_{O2}/P_0 < 2 ppm) to prevent mineral
113 oxidation. The hydrated and "pasty" outlayer of the core was firstly removed and the inner
114 sound part of the rock was kept. The inner core was then sliced using a wire saw into disk
115 samples with a thickness of ~ 10 mm, and a diameter of ~ 35-40 mm. The metrology of the
116 samples used in diffusion cells are provided in supplementary data (Table S2). These
117 measurements indicate an average hydrated density ~ 1.98 ± 0.10 g cm^{-3}. The difference

between this hydrated density and clay rock dry density ρ^{dry} ~ 1.7 g cm^{-3} provides a rough estimation of rock porosity: ε = 28 ± 10%. This value is in agreement with the results obtained from diffusion experiments detailed subsequently. Some of the remaining off-cut were crushed and sieved entirely below 125 µm for batch experiments.

A synthetic pore water was prepared by dissolution of pure salts (purity > 99.5%) to reach the composition for underground pore water of Gault formation clay rock (Ionic strength: IS = 2.33 10^{-2} M, equilibrated pH = 7.2 ± 0.2, Table S3). The synthetic water was bubbled (1 L min^{-1}) with a mix of N_2/CO_2 (99/1) for more than 2 hours, removing O_2 and equilibrating both dissolved CO_2. The synthetic pore water was then mixed with "sacrificial" crushed clay rock with a solid to liquid ratio of 10 g L^{-1} and agitated for more than 48 h. This step was used for the equilibration of trace elements such as Fe, Al, Mn, Si and NOM. Equilibrated pore water was filtrated through a 0.8 µm membrane to remove the sacrificial clay. Additional filtration step through a 0.22 µm membrane was processed before experiments to prevent bacterial activity. The composition of the equilibrated synthetic water was analysed by ionic chromatography (Metrohm, 850 IC). Alkalinity was measured by acidic dosage (HCOOH) in presence of methylene blue (Sarazin et al., 1999) with a UV-vis spectrophotometer (Cary-500 from Agilent). The prepared pore water was used for pre-equilibration step of clay samples, as described in the following section.

2.2. Adsorption experiments

The crushed clay (< 125 µm) was equilibrated for more than 48 hours with synthetic pore water in sealed polycarbonate centrifugation tubes, with a solid to liquid ratio of 250 g L^{-1} (1.5 g in 6 mL). Each tube was then spiked with ^{14}C or ^{3}H-organic tracer and agitated in a shaking machine for 24 h at least, and up to 7 days. At the time of sampling, the tubes were

centrifuged over 50,000 g for 1 h and a fraction of the supernatant was sampled. The tracer activity was determined by liquid scintillation counting on 1 mL samples (Packard TRICARB 2500), after addition of 4 mL of liquid scintillation solution (ultima gold^{TM} cocktail). The mass balance was checked for each tracer by duplicate experiments, i.e. without clay. The variation of blank activity was below measurement accuracy ($\Delta A_0 < 2$ %). All organic molecules studied in this work and their properties are displayed in Table 1. Aromatic and small carboxylic acids were chosen as compounds potentially released by degradation of graphite. The compounds were also chosen in order to cover a wide range of lipophilicity (-4 < log D < 3.5). The equilibrium concentration range was limited by the solubility of the organic compound in aqueous solution and the specific activity of radioactive sources. When available, full sorption isotherms cover a wide range of concentrations, thus providing information on sorption process, e.g. isotherm shape and saturation of sorption sites (Langmuir, Freundlich, etc.).

Table 1 Properties of organic molecules. P_{OW} is the octanol water partition coefficient of carboxylic acids (RCOOH). log P_{APP} is the apparent partition coefficient in Tégulines pore water (pH ~ 7.2). *$pH^{EXP.}$ = 7.7 ± 0.2. Recommended values are in bold. [$]Structure of molecules detailed in Table S4. [1]

Compound	Name (IUPAC)	Formula[$]	M_W (g mol^{-1})	pK_a[1]	Charge (pH 7.2)	log P_{OW}[2,3,4]	log P_{APP} (Théor.)	log P_{APP} (Exp.)
o-phthalate	Benzene-1,2-dicarboxylic acid	$C_8H_6O_4$	166.14	2.94, 5.43	$Ph.^{2-}$	0.73	-5.3	**-2.77** ± 0.2*
Oxalate	Oxalic acid	$C_2H_2O_4$	90.03	1.25, 4.14	$Ox.^{2-}$	-0.47	-9.5	**-3.96** ± 0.2*

(Haynes, 2014), [2] (Hansch et al., 1995), [3] (Pinsuwan et al., 1995), [4] (Sangster, 1989).

162	Benzoate	Benzoic acid	$C_7H_6O_2$	122.12	4.20	Bz^-	1.87	-1.13	**-1.26** ± 0.2*
	Adipate	Hexanedioic acid	$C_6H_{10}O_4$	146.14	4.43, 5.42	$Ad.^{2-}$	0.08	-4.5	n.d.
	Naphthalene	Naphthalene	$C_{10}H_8$	128.17	aprotic	N^0	3.32	3.4	**3.3** ± 0.1
	Toluene	Toluene	C_7H_8	92.14	aprotic	T^0	2.73	2.7	**2.77** ± 0.1
	Benzene	Benzene	C_6H_6	78.11	aprotic	B^0	2.13	2.1	**1.82** ± 0.1

2.3 Diffusion experiments

Six diffusion experiments were conducted in typical through-diffusion cells (numbering provided in Table 3), with a geometry detailed in Descostes et al., (2008) and provided in Fig. S3. Prior to diffusion experiments, the rock samples were pre-equilibrated by filling both upstream and downstream reservoirs with synthetic pore water. Clay was then equilibrated more than 48h and solutions renewed several times in order to ensure chemical equilibrium. Semi-heavy water (HDO) was used as a conservative reference, i.e. non sorbing tracer with access to the whole porosity. To that aim, upstream solutions were spiked with heavy water (D_2O). Both compartments were then periodically sampled. HDO content was measured by infrared laser spectrometry (LGR, DLT-100 from Los Gatos Research). After sampling, the upstream volume was refilled with initial injection solution and downstream volumes refilled with raw pore water. After a few weeks of monitoring, upstream solution was renewed by a solution with labelled organic tracers. The initial concentrations of organics were controlled by Total Organic Carbon analysis (Vario TOC Cube from Elementar) for cold solutions. Through-diffusion of organic compounds was monitored following the same procedure than for HDO, except that samples were measured by liquid Scintillation Counter (Packard TRICARB 2500 with ultima gold^{TM}, Perkin Elmer).

2.4 Data modelling

Distribution between liquid and solid may follow two mechanisms: absorption or adsorption. Absorption is a process in which an absorbate (atoms, molecules or ions) goes into a bulk phase of absorbent. The mechanism at the interface can be considered as a partitioning in two immiscible phases. Adsorption is a surface phenomenon, with an "increase in the concentration of a substance at the interface between a condensed material (sorbent) and in our case a liquid phase. Both absorption and adsorption can be quantified by a solid-liquid distribution coefficient, R_d (L kg^{-1}):

$$R_d = \frac{q_e}{C_e} \quad (1)$$

where q_e (mol kg^{-1}) is the concentration of sorbed species per mass of sorbent, and C_e (mol L^{-1}) the concentration in solution at equilibrium with the solid. In this work, the solid-liquid distribution coefficient R_d (L kg^{-1}) is calculated using the following Eq. (2):

$$R_d = \left(\frac{C_0}{C_{eq}} - 1\right) \times \frac{V}{m} = \left(\frac{A_0}{A_{eq}} - 1\right) \times \frac{V}{m} \quad (2)$$

with C_0/C_{eq} (mol L^{-1}) being the initial/equilibrium concentrations in solution; A (Bq) the activity, assumed proportional to C at any time; V (mL) the solution volume; and m (g) the dry mass of clay rock. The uncertainty (u) on R_d values is calculated using uncertainties on previous parameters through the Eq. (3):

$$u_{R_d}^2 = \left(\frac{V}{m \times A_{eq}}\right)^2 u_{A_0}^2 + \left(-\frac{A_0}{A_{eq}^2}\frac{V}{m}\right)^2 u_{A_{eq}}^2 + \left(\frac{R_d}{V}\right)^2 u_V^2 + \left(\frac{R_d}{m}\right)^2 u_m^2 \quad (3)$$

Sorption isotherms can be described by several empirical equations. For example, Langmuir and Freundlich isotherms are described by Eq. (4) and Eq. (5), respectively, with K_L (L mol^{-1}), K_F (L$^{(1/n)}$ kg^{-1} mol$^{(1-1/n)}$), the affinity constants, and Q (mol kg^{-1}) the maximum sorbed amount. Langmuir-type isotherm is usually observed when adsorption occurs with a single energy interaction, leading to surface monolayers. Such behavior was evidenced by adsorption of hydrophilic organic molecules on COx clay rock (Rasamimanana et al., 2017a). Freundlich isotherm is more common when several interactions occur, e.g. including multilayer or absorption processes. The parameter 1/n can be seen as a sorption intensity (Karnitz et al., 2007). When n = 1, the Freundlich isotherm, Eq. (5), becomes analogue to partitioning, $R_d = K_F = C_{org.}/C_{eq.}$. In this work, Eq. (4) and Eq. (5) are respectively applied to describe the adsorption of hydrophilic organic molecules and absorption of lipophilic organic molecules in Tégulines clay rock.

$$q_e = Q \times \frac{K_L \times C_e}{1 + K_L \times C_e} \quad (4)$$

$$q_e = K_F \times C_e^{1/n} \quad (5)$$

The one dimensional analysis of diffusion results is based on Fick's second law (Crank, 1975), described by Eq. (6):

$$\frac{\partial C}{\partial t} = \frac{D_e}{\varepsilon_a + \rho(1-\varepsilon)R_d} \frac{\partial^2 C}{\partial^2 x} = \frac{D_e}{\alpha} \frac{\partial^2 C}{\partial^2 x} \quad (6)$$

with C represents the tracer concentration (mol L^{-1}), t the time (s), D_e the effective diffusion coefficient (m^2 s^{-1}), ε and ε_a are the total and diffusion accessible porosities, ρ is the grain density of Tégulines clay rock (~1.7 kg L^{-1}), α = R×ε is called the rock capacity factor. The normalized flux of tracer, J^{NORM} (m^2 s^{-1}) is defined by Eq. (7):

$$J_{down}^{NORM}(t) = \frac{L}{C_0}\frac{dn_{\mathrm{down}}(t)}{S \times dt} \quad (7)$$

where dn_{down} is the quantity of tracer reaching the downstream reservoir (moles), per unit of time dt (s), and per sample surface S (m^2), L (m) the thickness of sample, and C_0 (moles m^{-3}) the initial upstream concentration.

The effective diffusion coefficient (D_e) and the rock capacity factor (α) are adjusted by least-square fitting of both downstream flux and depletion of the upstream concentration. The mass balance was assessed by comparison between upstream experimental data and modelling. Satisfactory mass balances, $\Delta C << 5\%$, were obtained for all experiments, except for toluene (Cell n° 6) which is discussed furtherly. Data and modelling for the reference tracer, HDO, are provided in Fig. S4. The average values of D_e and ε for HDO obtained from the 6 samples are $D_e = (1.38 \pm 0.37) \times 10^{-10}$ m^2 s^{-1} and $\varepsilon = 0.41 \pm 0.06$.

3. Results

3.1. Sorption of organic compounds on Tégulines clay

The Fig. 1 shows the experimental sorption results on Tégulines clay rock. R_d values of ionizable compounds are rather constant as a function of equilibrium concentration. The corresponding average value, R_d^{EXP}, for each organic compound are gathered in Table 2. Some compounds display significant affinities (i.e. $\rho \times R_d >> \varepsilon$). For example, the value R_d (oxalate) = 4.7 L kg^{-1} is one order of magnitude higher than that of benzoate.

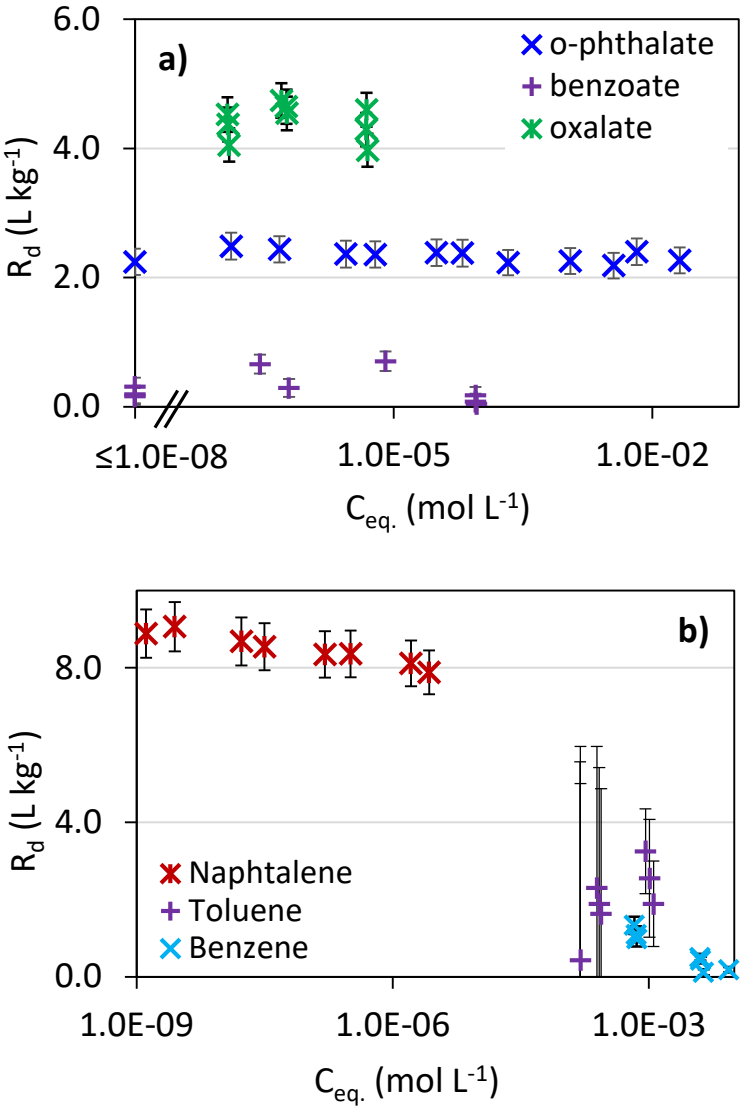

Fig. 1. Solid-liquid distribution coefficients (R_d) of organic compounds on Tégulines clay rock as a function of equilibrium concentration. V/m = 4 L kg^{-1}, pH = 7.2 ± 0.2, T = 22 ± 2°C.

(a) Data for ionizable compounds: o-phthalate, benzoate and oxalate.

(b) Data for neutral aromatic compounds: naphthalene, toluene and benzene.

The sorption isotherm of phthalate also displays a rather constant value. No clear saturation of sorption site is observed in the range of concentration measured, as expected in Langmuir-type shape (Eq. (4), Rasamimanana et al., 2017a). The best-fit modelling is provided in supplementary information (Fig. S2). Adjusted values are Q = 1.5 ± 2.1 mol kg^{-1},

and K_L = 1.6 ± 2.2 L mol^{-1}, leading to $R_d^{MAX} \sim K_L \times Q$ = 2.3 ± 4.5 L kg^{-1}. The o-phthalate compound displays higher affinity to Tégulines clay rock than benzoate. This highlights the role di-carboxylate group on sorption mechanism on the clay mineral surfaces (Rasamimanana et al., 2017a). Still, phthalate displays a weaker adsorption than oxalate, eventually linked to a steric effect, as discussed in Section 4.

Table 2 Solid-liquid distribution coefficients measured by batch experiments on Tégulines clay rock. pH = 7.2 ± 0.2, T = 22 ± 2 °C. V/m = 6 / 1.5 mL g^{-1}.

Compound	o-phthalate	Oxalate	benzoate	naphthalene	toluene	benzene
R_d (L kg^{-1})	2.33	4.65	0.55	9.10	2.57	1.14
± u(R_d)	± 0.10	± 0.10	± 0.23	± 0.23	± 0.68	± 0.18

The Fig. 1 also illustrate the sorption of neutral organic compounds on Tégulines clay rock. The R_d^{EXP} values of neutral organic compounds are displayed in Table 2, and exhibit with an order of naphthalene > toluene > benzene. The value R_d (naphthalene) = 9.1 L kg^{-1}, is one order of magnitude higher than that of benzene. These R_d values, from 1.14 to 9.10 L kg^{-1} are similar to that for ionizable compounds, despite rather different retention mechanism. Indeed, a slight decrease of R_d values is observed with the equilibrium concentration. Typical Freundlich isotherm, Eq. (5), was used to explain the naphthalene sorption isotherm, as illustrated in Fig. S2. The best fitting parameters are K_F = 6.9 ± 0.2 and n = 1.0. The value of the constant n = 1 indicates a constant energy interaction and a sorption mechanism such as absorption (i.e. partitioning between two phases). The constant value of R_d in this range of concentration allows the use of similar equations for both ionizable and neutral compounds for modelling of diffusion experiments.

3.2. Diffusion of organic compounds in Tégulines clay rock

The results of through-diffusion experiments are illustrate in Fig. 2. A depletion of upstream concentration and accumulation in downstream compartment (i.e. positive flux) is observed with time increasing. Phthalate was observed in the downstream during the first day, much earlier than adipate (~3 days) and oxalate (~15 days). This indicates a low retardation factor and retention for o-phthalate. On contrary, toluene was detected in the downstream after 14 days, indicating a higher retention. In the case of toluene, the non-linear sorption isotherm leads to a slight deviation between observed and model data and an "apparent" bias in mass balance. This does not affect significantly further estimation of the retardation factor, based on the normalized flux. For other compounds, the model agreement between both upstream and downstream data validates the model hypothesis, as well as mass balance of the experiment.

For all compounds, a "steady state" is reached after a few tens of days, meaning a constant flux of tracer. The normalized fluxes, calculated from downstream data with Eq. (7), are shown in Fig. 2. The value of the plateau provides a visual estimation of effective diffusion coefficients (D_e). The D_e of organic compounds in Tégulines clay rock ranges from 1 to 4 × 10^{-11} m^2 s^{-1}, with the order of phthalate < toluene < adipate < oxalate. These values are one order of magnitude lower than the effective diffusion of HDO. The adjustment of parameters D_e and α was performed using Eq. (7) by adjusting simultaneously both upstream and downstream data. The corresponding best fit values of D_e and α values are gathered in Table 3. The rock capacity factors ($\alpha = R\,\varepsilon$), sometimes referred as "apparent porosity", range from 0.47 (phthalate) to 7.72 (oxalate), higher than the total porosity quantified with HDO (ε = 0.41). This data quantifies the retention of the molecules during migration in Tégulines clay

315 rock. The corresponding solid-liquid distribution ratios calculated from Eq. 6 are discussed in
316 the following sections.

317 **Table 3** Reference of diffusion cell experiments, n°1 to 6. Corresponding diffusion parameters adjusted from experimental results (HDO for
318 water tracer). D_0 values are taken from Haynes (2014). *reprocessed to account for the experimental diffusion gradient.
319

Diffusion cell (**Tracer**)	IS (M)	D_e (water) (10^{-10} m^2 s^{-1})	*ε (water)*	*α* (org)	D_0(org) (10^{-10} m^2 s^{-1})	D_e(org) (10^{-12} m^2 s^{-1})	Π	R_d^{CELL} (L kg^{-1})	R_d^{BATCH} (L kg^{-1})
Cell n°1	0.02	1.04	0.41	0.47	6.96	10.05	0.32	0.16	2.33
^{3}H-phthalate		± 0.05	± 0.06	± 0.05		± 0.70	± 0.03	± 0.04	± 0.10
Cell n°2	0.02	1.43	0.45	0.64	6.39	23.63	0.58	0.30	-
^{3}H-adipate		± 0.16	± 0.06	± 0.10		± 2.70	± 0.10	± 0.08	
Cell n°3	0.02	1.65	0.47	7.58	9.87	36.44	0.52	5.93	4.65
^{14}C-oxalate		± 0.21	± 0.08	± 1.50		± 4.50	± 0.10	± 1.22	± 0.10
Cell n°4	0.32	0.96	0.34	5.59	9.87	23.32	0.57	4.31	-
^{14}C-oxalate	(phthalate)	± 0.05	± 0.05	± 1.20		± 4.70	± 0.11	± 0.97	
Cell n°5	0.32	1.93	0.46	11.12	9.87	40.84	0.50	8.80	-
^{14}C-oxalate	($NaNO_3$)	± 0.23	± 0.06	± 1.10		± 2.80	± 0.07	± 0.89	
Cell n°6	0.02	1.30	0.41	3.30	8.50	38.7*	0.82	2.45	2.57
^{3}H-toluene		± 0.04	± 0.05	± 0.80		± 3.6	± 0.8	± 0.65	± 0.68

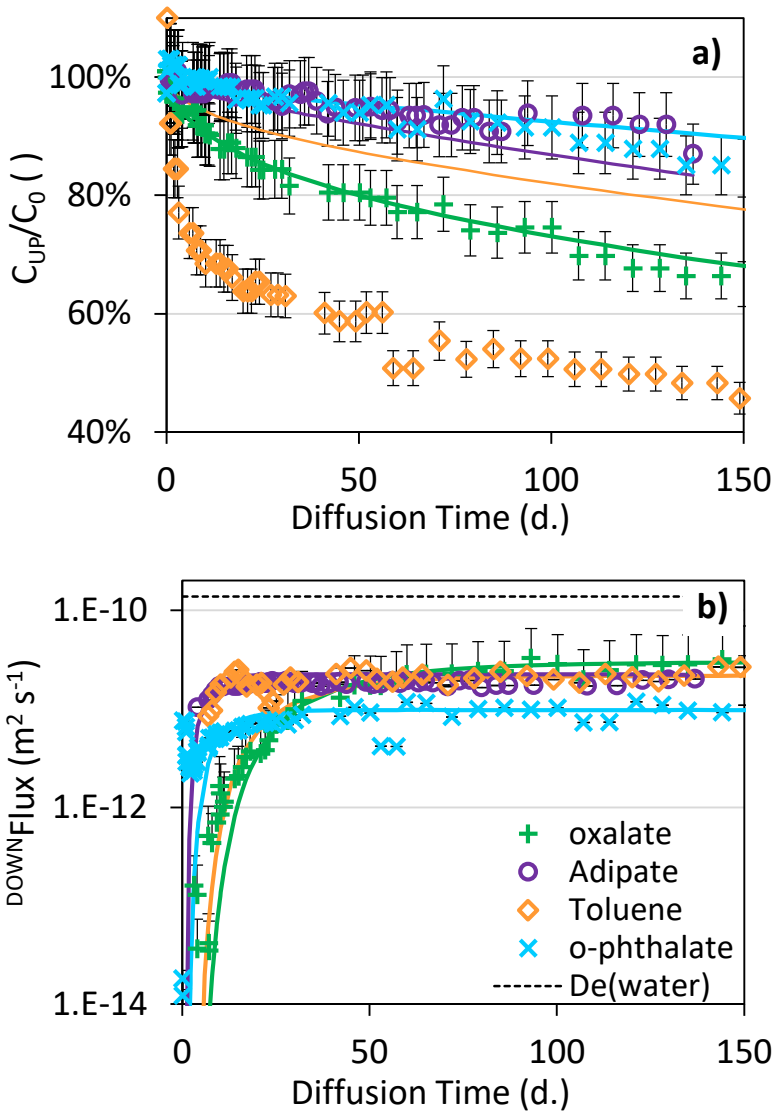

Fig. 2. Diffusion data of organic compounds in Tégulines clay rock. (a) Upstream concentration (b) Normalized Downstream flux. Solid lines represent best fit modelling (Upstream and downstream data adjusted simultaneously). Dashed line represents the average value measured for water, D_e (water) = (1.38 ± 0.37) × 10^{-10} m^2 s^{-1}.

3.4. Co-diffusion of organic and inorganic solutes

In order to get insights on the various mechanism occurring, e.g. anion exclusion and synergetic or competitive effects, the diffusion of oxalate was measured in presence of

345 organic and inorganic plumes. Additional through-diffusion experiments were performed with
346 ionic strength increased by an order of magnitude, i.e. from 2.33 10^{-2} M in Tégulines pore
347 water, up to 3.2 10^{-1} M. Ionic strength (IS = 0.32 M) was imposed by the presence of 0.1 M
348 sodium phthalate and 0.3 M $NaNO_3$ respectively. Diffusion data of oxalate under these
349 conditions are are provided in Fig. S6. The adjusted parameters, including D_e and α values,
350 are displayed in Table 3. Significant variation of D_e(oxalate) and α(oxalate) values are
351 observed in presence of saline and organic plume. Yet, the difference between both
352 experiments, i.e. o-phthalate and $NaNO_3$ plume, indicates that ionic strength is not the only
353 parameter affecting migration and anion exclusion. The transitory state during diffusion of
354 oxalate lasted ~ 15 days in raw Tégulines pore water. This transitory state was shorter (10
355 days) in presence of 0.3 M $NaNO_3$, while much longer (30 days) with addition of 0.1 M
356 sodium phthalate. Hence, both experiments at high ionic strengths induced opposite
357 disturbances compared to the "sound" state. These effects are quantified by the effective
358 diffusion coefficients, D_e, which is an indicator of charge or steric exclusion, and rock
359 capacity factor, α, which is an indicator of retention (Table 3). The possible mechanisms
360 occurring, e.g. anion exclusion or pH drift are reviewed in the following section.
361
362

4. Discussion

4.1 Retention of lipophilic compounds (log P_{OW} > 1)

The interaction between neutral aromatic compounds and soils is mainly related to absorption mechanism into NOM. Such hypothesis is easily assessed by representing the correlation between retention and lipophilicity of sorbates (Karickhoff et al., 1979). Lipophilicity of solutes is usually quantified by their octanol/water partition coefficient, P_{OW}. Strong correlations are observed between P_{OW} values and affinity on the NOM fraction of sorbents, i.e. $K_{OC} = R_d/f_{OC}$ (f_{OC} being the mass fraction of organic matter in the sorbent). Such correlation is illustrated in Fig. S7, with the corresponding linear regression $\log K_{OC} \sim 0.84 \times \log P_{OW} + 0.23$ ($R^2 = 0.84$). The slope of the curve: +0.84 traduces a thermodynamic equilibrium, with similar interactions involved in absorption and partitioning mechanisms, e.g. free enthalpy of solvation. The value $\log K_{OC} = +1.07$ (for $\log P_{OW} = +1$) quantifies a strength of interaction between slightly lipophilic solutes and NOM. On the other hand, the affinity between clay minerals and organic solutes is also well documented (Barré et al., 2014) and similar correlations due to hydrophobic interactions are expected (Willemsen et al., 2019). Yet, the correlations between retention and $\log P_{OW}$ are less obvious, as illustrated in Fig. S7, with $\log K_{CM} \sim 0.51 \times \log P_{OW} - 0.98$. The low correlation ($R^2 = 0.11$) and strong data disparity are caused by the diversity of phyllosilicates structures, as well as various adsorption mechanisms (Barré et al., 2014). Still, the value $\log K_{CM} = -0.47$ (for $\log P_{OW} = +1$) indicates an affinity of clay minerals, almost two orders of magnitude below the previous value for NOM. Hence, the two previous correlations are useful to assess, in a first macroscopic approach, the respective contributions of NOM and clay minerals to the retention in sedimentary rocks. Fig. 3 (a) illustrates the relative contributions of absorption in NOM and of adsorption on clay minerals in two examples of sedimentary rocks. The agreement between predicted values and experimental data on Tégulines ($f_{OC} \sim 0.5\%$, $f_{CM} \sim 50\%$) and OPA ($f_{OC} \sim$

388 0.8%, f_{CM} ~ 60%) clay rocks is rather good. The fact that clay minerals contribution displays a
389 lower slope than NOM contribution induces interesting features. The contribution of
390 absorption mechanism in NOM prevails for high values of log P_{OW}. This remains true even in
391 sedimentary rocks with low NOM content, such as Tégulines clay rock (f_{OC} = 0.5%, Lerouge
392 et al., 2018), OPA clay (f_{OC} = 0.5%, Wersin et al., 2008), or COx clay rock (f_{OC} = 0.6%,
393 Gaucher et al., 2004). On the other hand, the adsorption on phyllosilicates may control the
394 retention of solutes with low log P_{OW} values, especially for such rocks with high contents of
395 clay minerals (f_{CM} > 50%). As a corollary, the accurate measurement of low NOM content
396 (f_{OC} < 1%) provides a useful data, complementary to clay mineralogy. This allows to
397 determine sorbing phases and predict the migration of lipophilic compounds (dissolved gas,
398 pesticides, etc.) in sedimentary rocks and geobarriers.
399
400
401
402
403
404
405
406
407
408
409
410
411
412

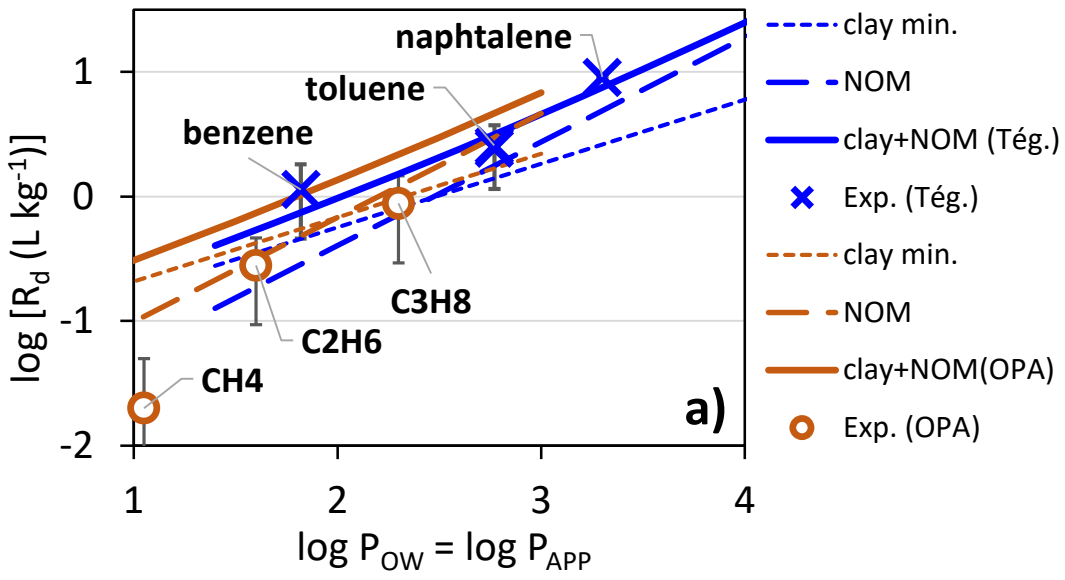

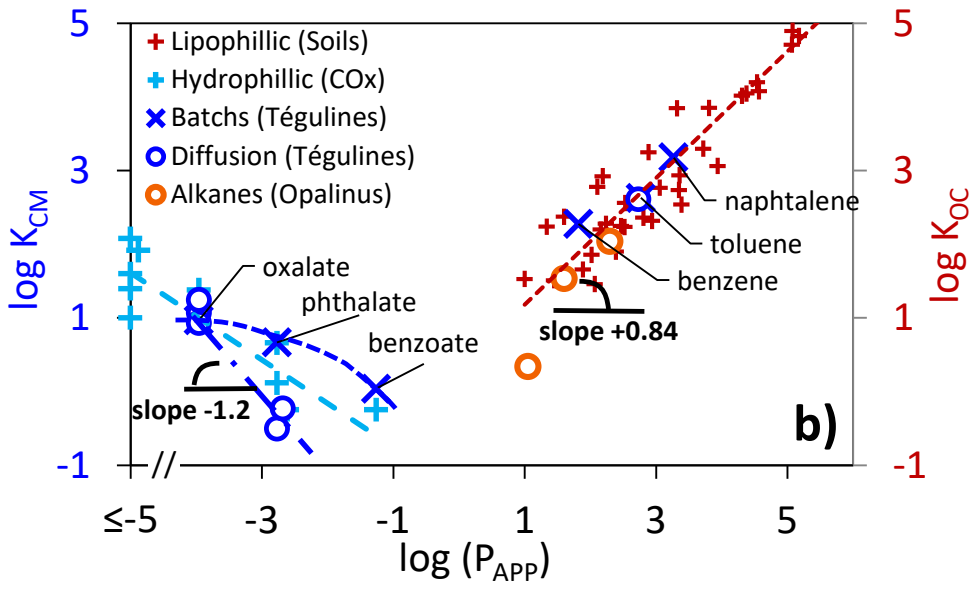

Fig. 3. Correlation between partition coefficient of organic compounds and their retention properties in natural media (near neutral pH ~7.2). a) Data for lipophilic compounds (log P_{APP} > 1) measured on Tégulines (Tég.) and Opalinus (OPA) clay rocks. Dashed lines: theoretical contribution expected from absorption in NOM and adsorption on phyllosilicates. Signs correspond to experimental data: Adsorption and through-diffusion in Tégulines at 22 ± 2°C (This work), In situ out-diffusion experiment in OPA at 16.5 ± 1.5°C (Vinsot *et al.*, 2017). b) Comparison of adsorption data for hydrophilic compounds ($K_{CM} = R_d/f_{CM}$) and absorption data of lipophilic compounds ($K_{OC} = R_d/f_{OC}$). Data on Tégulines (This work), OPA (Vinsot et al., 2017), COx clay rock (Rasamimanana et al., 2017a) and soils (Karickhoff et al., 1981).

4.2 Retention of hydrophilic compounds (log P_{APP} < -1)

Ionizable compounds are among the most widespread hydrophilic compounds. For carboxylates ($RCOO^-$), octanol/water apparent partition coefficient may be estimated from the value of carboxylic acids (RCOOH) using the Eq. 8 (Sangster, 1989):

$$P_{APP} = \frac{P_{OW}}{1 + 10^{(\mathrm{pH} - \mathrm{p}K_{a1})}} \quad (8)$$

437

438 However, such equation becomes unsuitable for highly hydrophilic compounds. For
439 that reason, log P_{APP} values were experimentally measured in this study. The methodology
440 and results are provided in supplementary material (Fig. S1). The corresponding values are
441 gathered in Table 1. As for hydrophilic compounds, a correlation is observed between log R_d
442 and log P_{APP} values of ionizable compounds (Fig. 3, b). In this case, the slope is negative,
443 which indicates a retention mechanism differing from that for aromatic compounds, i.e. more
444 likely an adsorption mechanism on surfaces of clayey minerals. Hence, R_d values are
445 normalized by the content of clay minerals in the media, $K_{CM} = R_d/f_{CM}$, in order to ease the
446 comparison between rocks. Results on Tégulines soft clay rock (Fig. 3, b) are in line with data
447 previously published on COx hard clay rock (Chen et al., 2018; Durce et al., 2015;
448 Rasamimanana et al., 2017b). A linear correlation is observed between retention of solutes
449 and hydrophilicity of sorbates ant that solvation and retention mechanism involve similar
450 interactions. Moreover, the value of the slope close to unity, (-1.2 ± 0.1), tends to indicate that
451 thermodynamic equilibrium is reached during diffusion experiments. Some correlation
452 between hydrophilicity of ionizable sorbates and retention has been previously reported on
453 COx clay rock, but without evidence of any sorption "maximum" (Rasamimanana et al.,
454 2017a). The correlation observed on Tégulines clay rock, K_{CM} = f(log P_{APP}), seems to point
455 out a rise to a plateau for highly hydrophilic sorbates, e.g. oxalate. This means that below a
456 certain value of log P_{APP}, the affinity between hydrophilic sorbates and minerals does not
457 increase "indefinitely". This trend differs from the affinity of lipophilic compounds which
458 increases up to log P_{OW} values over +6.

459 Speciation calculation are illustrated in supplementary material (Fig. S8). Data
460 indicates than the acidic form of solutes becomes negligible at near-neutral pH. Hence, the

retention mechanism may imply anionic species, rather than protonated organic acids. On the other hand, the relative contribution of mineralogical phases (especially clay minerals and oxides) to the retention of ionizable compounds deserves further numerical or experimental investigations (Ilina et al., 2020). For example, the presence of oxidized minerals in samples may contribute to differences between batch and diffusion experiments, as observed for o-phthalate and discussed furtherly.

4.3. Diffusion data and exclusion from rock porosity

The effective coefficients obtained from the diffusion experiments are lower than that of water, almost by an order of magnitude (Table 3). This behaviour is usually explained by a phenomenon of anion exclusion in surface charged media (de Haan, 1968). Such data can be discussed using the exclusion factor, Π, defined by Eq. 9:

$$\prod(\text{solute}) = \frac{D_e(\text{solute})/D_e(\text{water})}{D_0(\text{solute})/D_0(\text{water})} \quad (9)$$

where D_e is the effective diffusion coefficient in the porous solid and D_0 in water. The ratio D_e(solute)/D_e(water) quantifies the effect of clay rock on the diffusion of a solute, in comparison with non-reactive species such as water. This ratio is then normalized by D_0(solute)/D_0(water), in order to remove the contribution of solvent (poral water) on the diffusivity. Thus, the exclusion factor ∏ isolates the effect from the porosity of the media (i.e. tortuosity and constrictivity, Van Brakel and Heertjes, 1974) on the diffusion pathways of solutes. Fig. 4 shows the exclusion factor of anionic solutes as a function of their sizes (estimated from molecular mass). Data is reported for both COx and Tégulines clay rocks. Previous studies evidenced anion exclusion in COx clay rock for both inorganic (Descostes et al., 2008) and organic anions (Dagnelie et al., 2018), with exclusion factors down to 0.1 (i.e. Π(anion) << Π(water) = 1). This phenomena is usually explained by the presence of surface

charged clay minerals (Tournassat et al., 2016) and more pronounced when pore size is small (Gaboreau, et al., 2016; Wigger et al., 2018). For example, a strong anion exclusion is observed in COx clay units (UA2, UA3, <-450 m in depth), quantified with $\Pi(Cl^-/COx) \sim 0.3 \pm 0.1$ (Descostes et al., 2008). In contrast, no anion exclusion was evidenced with chloride in Tégulines soft clay rock, despite similar content in clay minerals. The absence of chloride exclusion in Tégulines, $\Pi(Cl^-/Tégulines) \sim 1$, can be explained by the shallow depth of the media: -75 m to -10 m (Debure et al., 2018). This leads to a less dense material ($\rho^{dry} \sim 1.7$ g cm^{-3}), and a limited diagenetic processes with pore diameters mainly higher than 30–50 nm (Lerouge et al., 2018).

Surprisingly, a significant exclusion was observed for organic molecules in Tégulines clay rock, thus differing from chloride case (Fig. 4, a). Regarding exclusion from porosity, the size of diffusing solutes may also decrease exclusion factor by steric effect, as clearly evidenced with neutral species, $\Pi(toluene/Tégulines) \sim 0.82 \pm 0.08$. The values for adipate and oxalate, $\Pi \sim 0.5 \pm 0.1$, are even lower than that of toluene (despite similar mass), indicating an additional contribution of charge to the exclusion from porosity. Still, the value of Π(organic anions) mainly decreases with the size of solutes (Fig. 4) for both Tégulines and COx clay rock. These trends indicate that the exclusion factors of complex anions is highly related to their sizes as compared to the size of pores in the media. Hard COx rock, with a pore size ~ 6-8 nm, displays a strong anion exclusion, even for chloride. Only small inorganic anion, such as Cl^-, display little exclusion factor in soft Tégulines rock (pore size ~ 20-30 nm). Since a significant exclusion is observed for larger species in both soft and hard rocks, other anions than Cl^- should be preferred to quantify exclusion factor of environmental media, e.g. NO_3^- SO_4^{2-}. These references, if conservative in the media, should be more representative of other contaminants such as AsO_4^{3-} or SeO_4^{2-}.

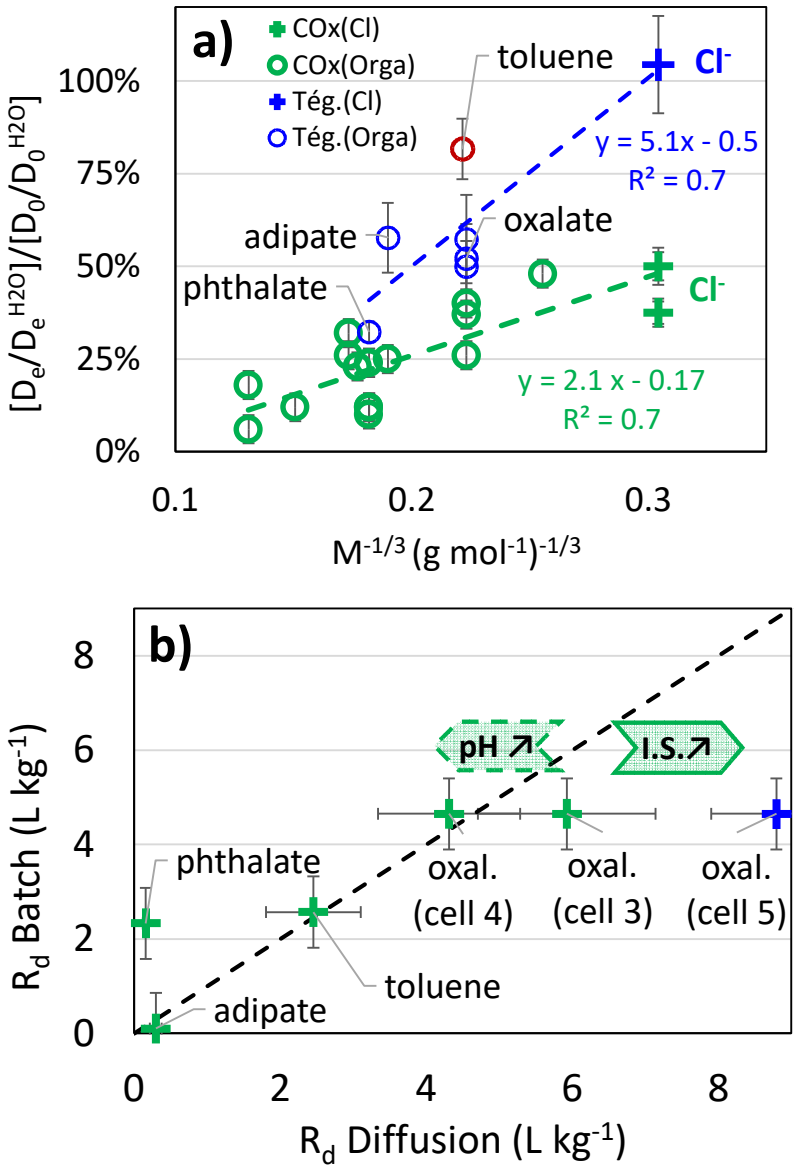

Fig. 4. Diffusion data for organic solutes. a) Exclusion factor for organic anions in COx clay rock (Dagnelie et al., 2014, 2018) and in Tégulines clay rock (Tég.) (This work). M: molecular mass. b) Solid-liquid distribution coefficient, R_d (L kg^{-1}), measured in Tégulines by batch experiments (X axis) and diffusion experiments (Y axis).

534 **4.4. Retardation and environmental implications**

535 Assessing the environmental impact of hazardous materials requires the estimation of
536 their migration properties, such as sorption, retardation and diffusivity. The predictive
537 migration modelling in natural media requires several building blocks. This includes accurate
538 description of the media, sorbing phases, and understanding of retention processes. It is then
539 useful to assess retention by various methodologies, e.g. molecular simulations, batch
540 experiments, migration experiments. This approach strengthen the description on underlying
541 phenomena and the accuracy on corresponding data. Such comparison of results is provided
542 in Fig. 4 (b). A large discrepancy is quantified between batch and diffusion data for slightly
543 lipophilic compounds, i.e. $-4 < \log P_{APP} < 0$, similarly to previous data on COx clay rock
544 (Dagnelie et al., 2018) or compacted clay minerals (Chen et al., 2018). This discrepancy is
545 especially striking for o-phthalate, for which diffusion data suggests strong steric and charge
546 exclusion. Similar observations on COx clay rock and illite suggest a "collapse" of retardation
547 when exclusion factor decreases below a "threshold" value. Yet, the mechanism leading to
548 such discrepancy is unclear. Further investigations are required to assess eventual hypotheses,
549 e.g. effect of anion exclusion on surface accessibility, oxidative perturbation of sulphide
550 minerals in crushed samples leading to additional (hydroxy)oxides, kinetic effects, etc.
551 Meanwhile, diffusion experiments and especially long-term *in situ* experiments seem
552 mandatory in order to accurately quantify the retardation factor of such solutes.

553

554 The batch and diffusion experiments provided consistent data for both toluene ($\log P_{APP} = 2.73$, lipophilic) and oxalate ($\log P_{APP} = -3.96$, hydrophilic). This validates the reactive
555 transport model, despite simplistic hypothesis (reversible and instantaneous retention) and the
556 absence of speciation calculations. The good agreement between results from both types of
557 experiments strengthens the accuracy on corresponding values: R_d (toluene/Tégulines) ~ 2.5 ±

559 0.3 L kg^{-1} and R_d (oxalate/Tégulines) ~ 4.5 ± 0.5 L kg^{-1}. Given the relatively good accuracy
560 on oxalate retention data, this later compounds was chosen for further co-diffusion
561 experiments. In the case of pollution events, the concomitant release of various contaminants
562 leads to co-sorption and co-diffusion phenomena. Several mechanisms may affect retention:
563 competitive sorption, pH drift, modification of IS, etc. In this context, diffusion of oxalate was
564 performed in presence of 0.1 M of o-phthalate (diffusion cell n°4) or 0.3 M of $NaNO_3$
565 (diffusion cell n°5). The retention of oxalate in sound sample (cell n°3), in presence of
566 phthalate (cell n°4), and in batch experiments, are in agreement with regard to the
567 uncertainties. This demonstrates that eventual pH drifts (between 7 and 9) due to the presence
568 of organic plume (Fralova et al., 2021) do not affect significantly diffusion. On contrary, a
569 slight increase of R_d(oxalate) is observed in presence of $NaNO_3$. This result may be linked to
570 the effect of ionic strength, which decreases anion exclusion, and thus increases accessibility
571 to surfaces and retardation. It is interesting to note that such an effect was not observed in cell
572 4, despite a similar ionic strength. This may probably be due to the diffusion speed of the
573 perturbation compared to oxalate diffusion. The effective diffusion coefficient of o-phthalate
574 is lower than that of oxalate. Thus in cell 4, the phtalate plume might diffuse too “slowly” to
575 affect significantly the diffusion of oxalate. Whereas in cell 5, the effective diffusion of NO_3^-,
576 which is faster than oxalate (Dagnelie et al., 2017), leads to an increase of IS along the
577 pathway of oxalate. Such effect may be responsible of the decrease of anion exclusion and
578 eventual increase of retention. This also confirms that oxalate exclusion is partially induced
579 by charge effects (in addition to steric effects), which is in agreement with measured
580 exclusion factors (i.e. Π(oxalate) < Π(toluene), Fig. 4). Overall, these results illustrate the
581 various mechanisms, with eventual antagonist effects, which may arise from release of
582 complex saline and organic plumes during pollution events.
583

584

585 **Conclusion**

586 Retention and diffusion of various organic compounds were quantified in the
587 Tégulines soft clay rock. A comparison is made with previous data measured on COx hard
588 clay rock. A significant affinity with clay rich rocks was observed for both lipophilic (log P_{OW}
589 > 1) and hydrophilic (log P_{APP} < -1) compounds. Neutral aromatic compounds mainly
590 undergo absorption mechanism in NOM. Such absorption is well correlated with the content
591 of NOM in the sorbent and the lipophilicity of the sorbate. The organic phase remains the
592 main sorbent for such compounds, even in media with low organic content, $f_{OC} \leq 0.6\%$. Still,
593 clay minerals may contribute to the retention of low lipophilicity compounds in such clay-rich
594 rocks ($f_{CM} \geq 40\%$). Nevertheless, the retention measured on crushed clay rock accurately
595 predict retardation measured by diffusion experiments. Additional mechanism of
596 intraparticulate diffusion should eventually be taken into account for migration modelling.

597 The ionizable compounds displayed values of solid-liquid distribution coefficients
598 similar to neutral compounds, but caused to adsorption mechanism. Surprisingly, this
599 adsorption was also correlated with the lipophilicity of solutes, with a maximum affinity
600 reached when log $P_{APP} \leq -4$. The diffusion data evidences an exclusion from rock porosity,
601 with a contribution of both size and charge of solutes. Such exclusion is higher for large
602 organic anions than for "small" inorganic anions such as chloride. The diffusive retardation of
603 solutes with intermediate polarities (log $P_{APP} \sim -2$), such as o-phthalate, was lower than
604 expected from batch experiments. Further studies would be interesting in order to quantify the
605 relative contribution of clay minerals and (hydroxy)oxides on the retention mechanisms.

606

607 **Acknowledgments**

608 This work was financed by CEA and the French radioactive waste management agency
609 (Andra).
610

References

Altmann, S., Tournassat, C., Goutelard, F., Parneix, J.C., Gimmi, T., Maes, N., 2012. Diffusion-driven transport in clayrock formations. Appl. Geochemistry 27, 463–478.

Andra, 2015. Projet de stockage des déchets radioactifs de faible activité massique à vie longue (FAVL) – Rapport d'étape 2015. FRPADPG150010.

Amédro, F., Matrion, B., Deconinck, J.-F., Huret, E., Landrein, P., 2017. Les forages de Juzanvigny (Aube, France): litho-biostratigraphie des formations du Barrémien à l'Albien moyen dans l'est du bassin de Paris et datations par les ammonites. Geodiversitas 39, 185–212.

Appelo, C.A.J., Van Loon, L.R., Wersin, P. 2010. Multicomponent diffusion of a suite of tracers (HTO, Cl, Br, I, Na, Sr, Cs) in a single sample of Opalinus Clay. Geochim. Cosmochim. Acta 74, 1201–1219.

Barré, P., Fernandez-Ugalde, O., Virto, I., Velde, B., Chenu, C. 2014. Impact of phyllosilicate mineralogy on organic carbon stabilization in soils: incomplete knowledge and exciting prospects. Geoderma 235–236, 382–395.

Borisover, M.D., Graber, E.R., 1997. Specific interactions of organic compounds with soil organic carbon. ACS Div. Environ. Chem. Prepr. 37, 172–174.

Borisover, M., Davis, J.A., 2015. Adsorption of Inorganic and Organic Solutes by Clay Minerals. Dev. Clay Sci. 6, 33–70.

Van Brakel, J., Heertjes. P.M., 1974. Analysis of Diffusion in Macroporous Media in Terms of a Porosity, a Tortuosity and a Constrictivity Factor. International Journal of Heat and Mass Transfer 17 (9), 1093–1103.

Chen, Y., Glaus, M.A., Van Loon, L.R., Mäder. U., 2018. Transport of Low Molecular Weight Organic Compounds in Compacted Illite and Kaolinite. Chemosphere 198, 226–37.

Crank, J. 1975. The Mathematics of Diffusion. London: Clarendon Press.

Dagnelie, R.V.H., Descostes, M., Pointeau, I., Klein, J., Grenut, B., Radwan, J., Lebeau, D., Georgin, D., Giffaut, E., 2014. Sorption and diffusion of organic acids through clayrock: comparison with inorganic anions. J. Hydrol. 511, 619–627.

638 Dagnelie, R.V.H., Arnoux, P., Enaux, J., Radwan, J., Nerfie, P., Page, J., Coelho, D., Robinet, J.-C.,
639 2017. Perturbation induced by a nitrate plume on diffusion of solutes in a large-scale clay rock sample.
640 Appl. Clay Sci. 141, 219–226.
641 Dagnelie, R.V.H., Rasamimanana, S., Blin, V., Radwan, J., Thory, E., Robinet, J.-C., Lefèvre, G.,
642 2018. Diffusion of Organic Anions in Clay-Rich Media: Retardation and Effect of Anion Exclusion.
643 Chemosphere 213, 472–80.
644 Debure, M., Tournassat, C., Lerouge, C., Madé, B., Robinet, J.-C., Fernández, A.M., Grangeon, S.,
645 2018. Retention of Arsenic, Chromium and Boron on an Outcropping Clay-Rich Rock Formation (the
646 Tégulines Clay, Eastern France). Sci.Total Environ. 642, 216–29.
647 Descostes, M., Blin, V., Bazer-Bachi, F., Meier, P., Grenut, B., Radwan, J., Schlegel, M.L.,
648 Buschaert, S., Coelho, D., Tevissen. E., 2008. Diffusion of Anionic Species in Callovo-Oxfordian
649 Argillites and Oxfordian Limestones (Meuse/Haute-Marne, France). Appl. Geochem. 23, 655–77.
650 Durce, D., Bruggeman, C., Maes, N., Van Ravestyn, L., Brabants, G. 2015. Partitioning of organic
651 matter in Boom Clay: Leachable vs mobile organic matter. Appl. Geochem. 63, 69–181.
652 Fralova, L., Lefèvre, G, Madé, B., Marsac, R., Thory, E., Dagnelie, R.V.H. Effect of organic
653 compounds on the retention of radionuclides in clay rocks: Mechanisms and specificities of Eu(III),
654 Th(IV), and U(VI). Appl. Geochem. 104859, 2021.
655 Gaboreau, S., Robinet, J.-C., Prêt. D. 2016. Optimization of Pore-Network Characterization of a
656 Compacted Clay Material by TEM and FIB/SEM Imaging. Microporous and Mesoporous Mater. 224,
657 116–128.
658 Gaucher, E., Robelin, C., Matray, J.-M., Négrel, G., Gros, Y., Heitz, J.F., Vinsot, A., Rebours, H.,
659 Cassagnabère, A., Bouchet, A., 2004. ANDRA underground research laboratory: interpretation of the
660 mineralogical and geochemical data acquired in the Callovian–Oxfordian formation by investigative
661 drilling. Phys. Chem. Earth, 29, 55–77.
662 Gu, B., Schmitt, J., Chen, Z., Liang, L., McCarthy, J.F., 1994. Adsorption and Desorption of Natural
663 Organic Matter on Iron Oxide: Mechanisms and Models. Environ. Sci. Technol. 28, 38–46.
664 de Haan, F.A.M., 1968. The Negative Adsorption of Anions (Anion Exclusion) in Systems with
665 Interacting Double Layers. J. Phys. Chem. 68 (10), 2970–2977.

Hansch, C., Leo, A., Hoekman, D., 1995. Exploring QSAR. Hydrophobic, electronic, and steric constants. ACS Professional Reference Book. ACS, Washington.

Haynes, W.M. (Ed.), 2014. CRC Handbook of Chemistry and Physics, 95th Edition, CRC Handbook of Chemistry and Physics, 95th Edition. CRC press.

Hwang, Y.S., Liu, J., Lenhart, J.J., Hadad. C.M., 2007. Surface Complexes of Phthalic Acid at the Hematite/Water Interface. J. Colloid Interface Sci. 307 (1), 124–34.

Ilina, S.M., Maran, L., Lourino-Cabana, B., Eyrolle, F., Boyer, P., Coppin, F., Sivry, Y., Gélabert, A., Johnson, S.B., Yoon, T.H., Slowey, A.J., Brown, G.E., 2004. Adsorption of organic matter at mineral/water interfaces: 3. Implications of surface dissolution for adsorption of oxalate. Langmuir 20, 11480–11492.

Kang, S., Xing, B., 2007. Adsorption of Dicarboxylic Acids by Clay Minerals as Examined by in Situ ATR-FTIR and Ex Situ DRIFT. Langmuir 23 (13), 7024–31.

Karickhoff, S.W., Brown, D.S., Scott. T.A., 1979. Sorption of Hydrophobic Pollutants on Natural Sediments. Water Research 13 (3), 241–48.

Karickhoff, S.W., 1981. Semi-empirical estimation of sorption of hydrophobic pollutants on natural sediments and soils. Chemosphere, 10 (8), 833–846.

Karnitz, O., Gurgel, L.V.A., de Melo, J.C.P., Botaro, V.R., Melo, T.M.S., de Freitas Gil, R.P., Gil, L.F., 2007. Adsorption of heavy metal ion from aqueous single metal solution by chemically modified sugarcane bagasse. Bioresour. Technol. 98, 1291–1297.

Lerouge, C., Robinet, J.C., Debure, M., Tournassat, C., Bouchet, A., Fernández, A.M., Flehoc, C., Lerouge, C., Debure, M., Henry, B., Fernandez, A. M., Blessing, M., Proust, E., Madé, B., Robinet, J. C. 2020. Origin of dissolved gas (CO_2, O_2, N_2, alkanes) in pore waters of a clay formation in the critical zone (Tégulines Clay, France). Appl. Geochem. 104573.

Maes, N., Bruggeman, C., Govaerts, J., Martens, E., Salah, S., Van Gompel, M. 2011. A consistent phenomenological model for natural organic matter linked migration of Tc(IV), Cm(III), Np(IV), Pu(III/IV) and Pa(V) in the Boom Clay. Phys. Chem. Earth 36, 1590–1599.

Melkior, T., Yahiaoui, S., Thoby, D., Motellier, S., Barthès, V., 2007. Diffusion coefficients of alkaline cations in Bure mudrock. Phys. Chem. Earth 32, 453–462.

694 Missana, T., Colàs, E., Grandia, F., Olmeda, J., Mingarro, M., García-Gutiérrez, M., Munier, I.,
695 Robinet, J.C., Grivé, M., 2017. Sorption of radium onto early cretaceous clays (Gault and Plicatules
696 Fm). Implications for a repository of low-level, long-lived radioactive waste. Appl. Geochemistry 86,
697 36–48.
698 Pageot, J., Rouzaud, J.N., Gosmain, L., Deldicque, D., Comte, J., Ammar, M.R., 2016. Nanostructural
699 characterizations of graphite waste from French gas-cooled nuclear reactors and links with 14C
700 inventory. Carbon N. Y. 105, 77–89.
701 Pageot, J., Rouzaud, J.N., Gosmain, L., Duhart-Barone, A., Comte, J., Deldique, D., 2018. 14C
702 selective extraction from French graphite nuclear waste by CO2 gasification. Progress in Nuclear
703 Energy, 105, 279–286.
704 Pignatello, J.J., Xing, B., 1996. Mechanisms of slow sorption of organic chemicals to natural particles.
705 Environ. Sci. Technol. 30 (1), 1–11.
706 Pinsuwan, S., Li, A., Yalkowsky, S.H., 1995. Correlation of Octanol/Water Solubility Ratios and
707 Partition Coefficients. J. Chem. Eng. Data 40, 623–626.
708 Poncet, B., Petit, L., 2013. Method to assess the radionuclide inventory of irradiated graphite waste
709 from gas-cooled reactors. J. Radioanal. Nucl. Chem. 298, 941–953.
710 Rasamimanana, S., Lefèvre, G., Dagnelie, R.V.H., 2017a. Adsorption of Polar Organic Molecules on
711 Sediments: Case-Study on Callovian-Oxfordian Claystone. Chemosphere 181, 296–303.
712 Rasamimanana, S., Lefèvre, G., Dagnelie, R.V.H., 2017b. Various Causes behind the Desorption
713 Hysteresis of Carboxylic Acids on Mudstones. Chemosphere 168, 559–67.
714 Sangster, J., 1989. Octanol-water partition coefficient of simple organic compounds. J. Phys. Chem.
715 Ref. Data 18 (3), 1111–1227.
716 Sarazin, G., Michard, G., Prevot F., 1999. A rapid and accurate spectroscopic method for alkalinity
717 measurements in sea water samples. Water Res. 33 (1), 290–294.
718 Savoye, S., Frasca, B., Grenut, B., Fayette, A., 2012. How mobile is iodide in the Callovo-Oxfordian
719 claystones under experimental conditions close to the in situ ones? J. Contam. Hydrol. 142–143, 82–
720 92.

721 Schaffer, M., Licha, T., 2015. A framework for assessing the retardation of organic molecules in
722 groundwater: Implications of the species distribution for the sorption-influenced transport. Sci. Total
723 Environ. 524–525, 187–194.
724 Shackelford, C.D., Moore, S.M., 2013. Fickian diffusion of radionuclides for engineered containment
725 barriers: Diffusion coefficients, Porosities, And complicating issues. Eng. Geol. 152, 133–147.
726 Tournassat, C., Gaboreau, S., Robinet, J.-C., Bourg, I.C., Steefel, C.I., 2016. Impact of microstructure
727 on anion exclusion in compacted clay media. The Clay Minerals Society Workshop Lectures Series,
728 21 (11), 137–149.
729 Vinsot, A., Anthony, C., Appelo, J., Lundy, M., Wechner, S., Cailteau-Fischbach, C., de Donato, P.,
730 Pironon, J., Lettry, Y., Lerouge, C., De Cannière, P. 2017. Natural Gas Extraction and Artificial Gas
731 Injection Experiments in Opalinus Clay, Mont Terri Rock Laboratory (Switzerland). Swiss Journal of
732 Geosciences 110 (1), 375–90.
733 Wersin, P., Soler, J.M., Van Loon, L., Eikenberg, J., Baeyens, B., Grolimund, D., Gimmi, T.,
734 Dewonck, S., 2008. Diffusion of HTO, Br−, I−, Cs+, 85Sr2+ and 60Co2+ in a clay formation: Results
735 and modelling from an in situ experiment in Opalinus Clay. Applied Geochem. 23, 4, 678-691.
736 Wigger, C., Gimmi, T., Muller, A., Van Loon, LR. 2018. The Influence of Small Pores on the Anion
737 Transport Properties of Natural Argillaceous Rocks – A Pore Size Distribution Investigation of
738 Opalinus Clay and Helvetic Marl. Appl. Clay Sci. 156, 134–143.
739 Willemsen, J.A.R., Myneni, S.C.B., Bourg, I.C. 2019. Molecular dynamics simulations of the
740 adsorption of phthalate esters on smectite clay surfaces. J. Phys. Chem. C, 123, 13624-13636.

Graphical Abstract